Anticyclones drive Beaufort breakout events

MacKenzie E. Jewell[1], **Jennifer K. Hutchings**[1]

[1]College of Earth, Ocean, and Atmospheric Sciences, Oregon State University, 104 CEOAS Administration Building, Corvallis, OR 97331, USA

Key Points:

- Observational data provide context for a 2013 Beaufort Sea breakout recently simulated with the neXtSIM model by Rheinlænder et al. (2022)
- While the 2013 event was exceptional, winter breakouts are common under anticyclonic winds including in years when the ice was thicker
- Wind direction is the primary control on the location of lead opening and the transition to breakout in the Beaufort Sea

Corresponding author: MacKenzie E. Jewell, `jewellm@oregonstate.edu`

Abstract

In winter 2013, a sea ice breakout in the Beaufort Sea produced extensive fracturing and contributed to record regional ice export. Rheinlænder et al. (2022) simulated this event using the neXtSIM sea ice model, reproducing a realistic progression of lead opening and ice drift following the track of an anticyclone. In their study, Rheinlænder et al. (2022) highlighted strong winds and thin ice as key factors for breakouts. We draw on observational records to provide additional context for the driving mechanisms of breakout events. We show that wind direction, rather than speed, was the primary control on patterns of lead opening and breakout timing in 2013. Records of similar events over previous decades demonstrate that breakouts are common under anticyclonic forcing, including during years when the ice was thicker. These additional events can be used to further validate models such as neXtSIM and improve predictive capabilities for future breakouts.

Plain Language Summary

In winter, the Beaufort Sea is covered by a layer of sea ice that is usually frozen against its coastal boundaries. When winds continuously blow from east to west over the sea, the ice cover can break apart and rapidly drift away from the coasts in what is called a breakout event. The prediction of such dynamic events is important for those who navigate the region. Rheinlænder et al. (2022) recently used the neXtSIM sea ice model to simulate and reproduce realistic ice cracking and drift during an exceptionally strong breakout that occurred in 2013. Rheinlænder et al. (2022) highlighted strong winds and thin sea ice as key factors for breakout. We use observational records to provide additional context for the drivers of Beaufort breakout events. Weather analysis shows that wind direction, rather than wind speed, was the primary control on breakout timing in 2013. Records of many similar events, including during years when the ice was thicker than in 2013, demonstrate that breakouts are common under weather patterns that produce east-to-west winds. These additional observed events can be used to assess and refine the performance of models such as neXtSIM to improve predictions of future breakouts.

1 Introduction

In winter, the Arctic Ocean is covered by a consolidated ice pack bounded by the Arctic coastline. The ice moves in response to winds and ocean currents, the response being regulated by stress transmission in the ice itself due to ice-coast interactions. When the ice pack moves away from the coast and experiences sustained drift out of the region and extensive lead opening, this is considered a breakout event. Predicting breakouts is of importance to those navigating or working in the consolidated ice pack.

During 2013 a sea ice breakout in the Beaufort Sea attracted public attention when it was reported in a popular blog (*The cracks of dawn*, 2013). This event has been simulated with the neXtSIM model by Rheinlænder et al. (2022). They find the location and timing of lead opening during the breakout is sensitive to choice of atmospheric model used to provide forcing for the sea ice. To our knowledge this is the first time lead opening and subsequent breakout of Beaufort Sea ice has been simulated with an accuracy that may allow synoptic forecasts suitable for predicting risk of cracking and lead opening around an ice camp, for example.

In this comment to Rheinlænder et al. (2022) we highlight the atmospheric synoptic conditions that drive the breakout and explain the relationship between anticyclone track and the formation of wide leads visible in satellite imagery. We point out that it is primarily the wind direction, rather than wind speed, which controls the patterns of lead opening and when breakout occurs. The 2013 event is put into the context of sim-

ilar events in the satellite record, including winters when the Beaufort Sea ice pack was thicker, identifying several case studies that could be used to verify models such as neXtSIM.

2 Typical breakout sequence

During winter and spring, anticyclones repeatedly travel eastward over the Beaufort Sea activating leads from west to east along the Alaskan coast. The leads typically extend offshore toward the center of the passing anticyclone, bounding regions of enhanced fracturing (breakup) and ice drift where the ice pack loses contact with the coast.

Common lead patterns include small scale arches called Beaufort Arches (BA) (Figure 1a) and large arched leads called Tangent Arcs (TA) (Figure 1b-d) that extend from Point Barrow, Alaska under northeasterly winds. Wide Angle (WA) (Figure 1f) then High Angle (HA) (Figure 1g) leads extend offshore from the central and eastern coast of the Alaska North Slope, respectively, as winds shift westward. If winds shift offshore, an East Coastal (EC) flaw lead (Figure 1e-h) opens parallel to Banks Island at the eastern boundary of the Beaufort Sea. This marks the transition to breakout. The entire ice pack detaches from its coastal boundaries and accelerates until offshore wind forcing weakens. The relationship between opening of coast-originating lead patterns and anticyclone position is further detailed in Supplementary Text S1.

As Beaufort breakouts are driven by easterly winds associated with high sea level pressure over the Beaufort Sea, a strong and persistent meridional pressure gradient can signal the forcing required to initiate most breakouts. Breakouts are characterized by large ice drift speeds, ice export from the Beaufort Sea, and extensive breakup of the ice pack. These metrics, as well as the opening and persistence of Alaska coastal then EC flaw leads, indicate that breakout has occurred.

3 The 2013 Beaufort breakout

From late February through early March of 2013, high sea level pressure and anticyclonic winds persisted over the Pacific Arctic. Under this continuous forcing, a series of leads opened along the Beaufort coast and progressed eastward, resulting in a breakout event (Figure 1 and Supporting Information Movie S1).

Preceding breakout, an anticyclone over the East Siberian Sea opened BA leads from February 12 - 14 (Figures 1a, 2a). By February 15, the high pressure system moved south toward the Chukchi Sea, opening a TA lead that extended further offshore than the existing leads (Figure 1b). Most of the Beaufort Sea ice pack remained stationary while ice downwind of the lead accelerated and fractured. Ice drift temporary slowed as the high migrated northeastward, reducing wind speeds to near-zero over the lead. By February 20, the high stalled near $80°N$, $160°W$ and a northeasterly wind returned over the dormant TA lead (Figure 2b). Additional TA leads opened upwind as ice flushed from the Beaufort Sea (Figure 1c). On February 21, the longest TA lead of this event extended nearly 800 km offshore from Point Barrow, aligned with the northeast wind. Ice drifted southwestward along the lead, bounded upwind by a secondary lead extending northward nearly perpendicular to the primary fracture and the direction of ice drift. Additional fractures extended westward, terminating near the center of the anticyclone and completing the characteristic arch shape of TA leads.

On February 24, the anticyclone's orientation began to shift. The wind speed and meridional pressure gradient remained constant (Figure 2b,c), but wind direction shifted westward. This increase in alongshore wind forcing overcame the strength of the ice previously buttressed by the coast on the windward side of the TA lead. A cascade of WA and HA leads opened along the coast as the high continued to rotate then traveled eastward (Figure 2d,e). Finally, on February 27, winds shifted slightly northward (Figure

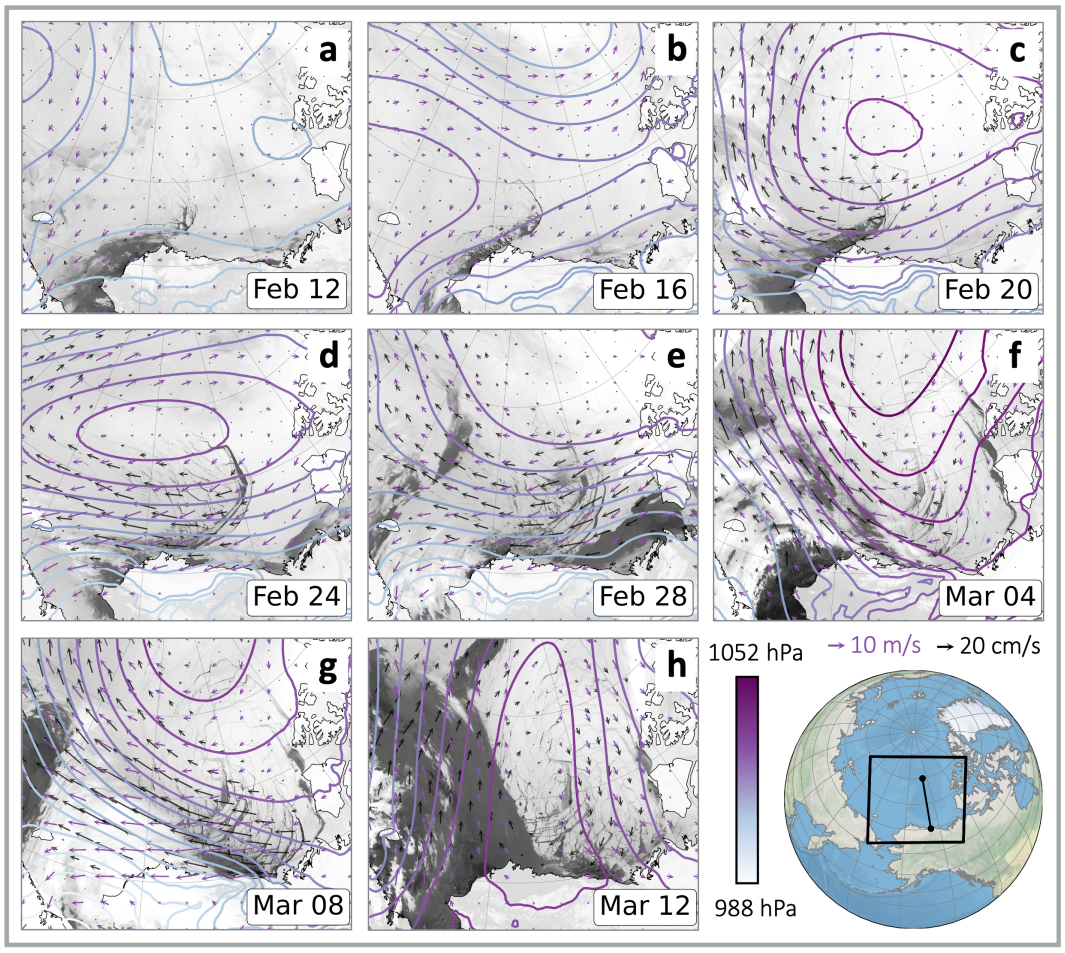

Figure 1. Thermal infrared MODIS imagery (Band 31) of Beaufort Sea during 2013 breakout (region outlined in black box on inset map). Daily average ERA5 10 meter winds shown as purple arrows and sea level pressure contours overlain every $4\,hPa$ (Hersbach et al., 2018). Black arrows are NSIDC daily ice drift (Tschudi et al., 2019). Black line on inset map shows $70°N - 80°N$ along $145°W$ (used in calculations).

2b) and the remaining coastally-bound ice broke loose as an EC lead developed. A large sea level pressure gradient and easterly wind remained through March 9. Under this sustained forcing, the EC lead persisted for two weeks alongside heavy breakup and rapid ice drift (Figure 2a).

4 Is this an unusual event?

Breakouts are common in winter (here defined as January-April), and the sequence of lead opening and rate of ice flux during the 2013 breakout were comparable to events from other years. However, the record persistence of synoptic forcing in 2013 resulted in exceptional ice dynamics. The 2013 breakout produced the second most persistent winter EC lead of the previous two decades (Lewis & Hutchings, 2019) and contributed to the largest March ice flux out of the Beaufort Sea from 1979-2016 (Babb et al., 2019).

Beginning February 21, the meridional sea level pressure difference (ΔP) between $70°N - 80°N$ along $145°W$ exceeded $20\,hPa$ for 10 consecutive days (Figure 2c). Fig-

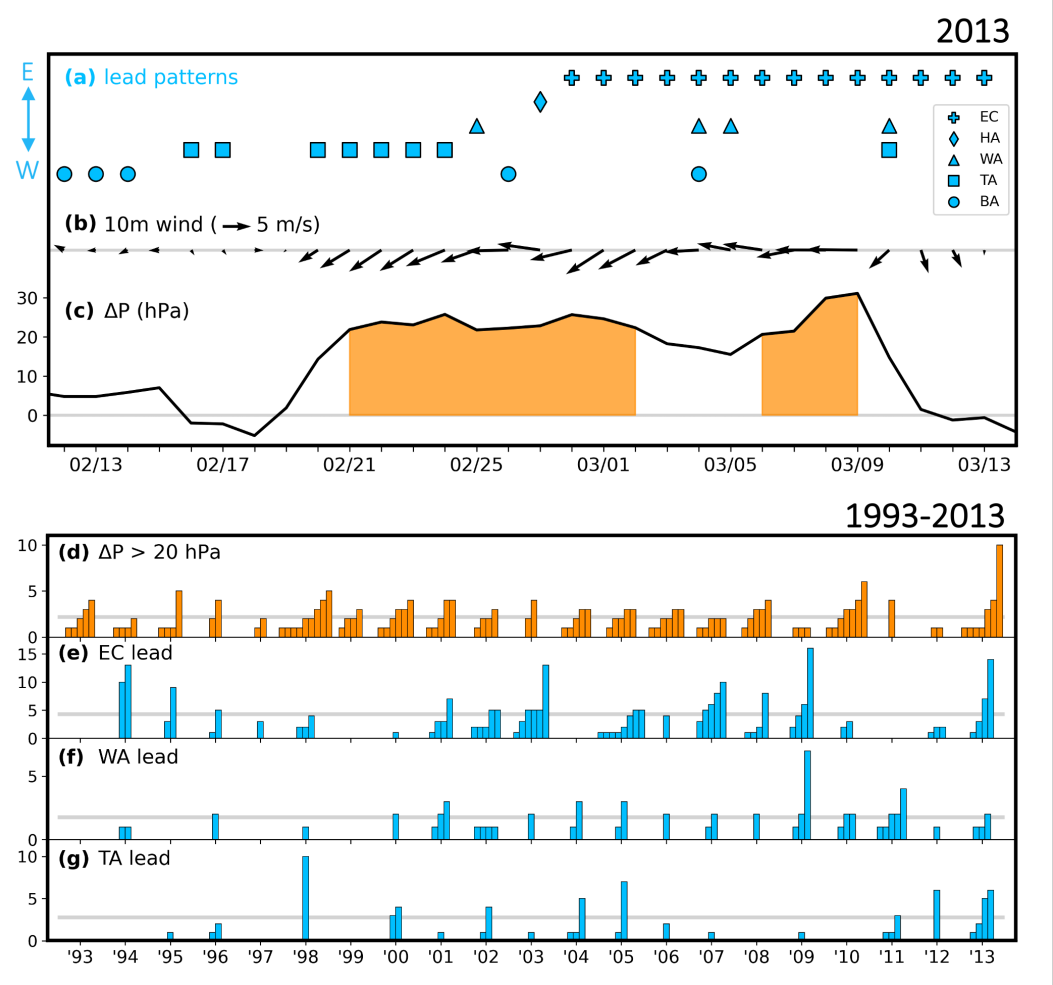

Figure 2. **Top:** 2013 breakout event. (a) Leads identified by Lewis and Hutchings (2019), arranged from westernmost to easternmost patterns. BA leads include Wide BAs and HA leads include HA fans, defined in Lewis and Hutchings (2019). Daily ERA5 atmospheric conditions along $145°W$: (b) average 10 meter winds between $70°N - 80°N$ and (c) sea level pressure difference between $70°N - 80°N$ (ΔP). $\Delta P > 20\,hPa$ highlighted in orange. **Bottom:** Occurrence of $\Delta P > 20\,hPa$ (d) and specified lead patterns (e-g) from January-April 1993-2013 (Lewis & Hutchings, 2019). Each bar represents an occurrence. Bar height indicates duration. Grey lines show mean durations.

ure 2d shows the occurrence and persistence of $\Delta P > 20\,hPa$ during winters 1993-2013. While other winters exceeded the $20\,hPa$ threshold for a comparable number of days overall (e.g. 1998, 2010), the 2013 synoptic event lasted 5 times longer than average and was the longest of the last 4 decades (Supplementary Table S1 lists dates of comparable synoptic events 1979-2022). During the breakout, more than $100,000\,km^2$ of sea ice was exported from the Beaufort Sea during the last week of February and the first week of March (Babb et al., 2019). The rate of ice flux during this period was comparable to events in earlier years (e.g. 1998 and 2008 in Figure 12 of Babb et al. (2019)). Thus, the exceptional ice loss owed to the persistence of forcing over this period.

TA, WA, and EC leads were the most common lead patterns during the transition to breakout in 2013. While the WA lead was not especially persistent, both the TA and EC leads opened for longer than average (for 5 and 14 consecutive days, respectively). Comparable events have occurred throughout the satellite record including during years when the ice pack was thicker than in 2013 (Figure 2e-g). Supplementary Table S2 lists dates of comparable lead sequences from 1993-2013 as identified by Lewis and Hutchings (2019). These events could serve as similar cases for simulation with neXtSIM and other models.

Rheinlænder et al. (2022) demonstrated that neXtSIM simulations initialized with thinner ice resulted in increased lead fraction and ice velocity. While this indicates that thinning ice increases the dynamic response of the ice pack to winds during breakout in the model, thin ice is not required to initiate breakout. When the initial ice thickness was doubled relative to the primary neXtSIM simulation, breakout still resulted under the same forcing (Supplementary Figure S4), though the ice drift speed decreased. Considering this and similar events from previous decades when the ice was thicker, ice thickness likely influences breakout strength more so than frequency, which is primarily controlled by the frequency of anticyclonic forcing.

5 Discussion

While the synoptic conditions and ice dynamics of the 2013 breakout were exceptional, periods of enhanced ice drift and breakup associated with lead opening or breakout events are frequent throughout winter. The location of lead opening determines the position of ice acceleration as the ice pack separates from the coast. Thus, lead location and the direction and speed of ice drift are each important metrics for assessing the skill of a sea ice model for use in forecasting ice conditions.

The neXtSIM model has demonstrated remarkable accuracy in simulating the dynamics associated with the 2013 event. The model appears to produce a range of Beaufort Sea lead patterns associated with breakout, and the episodic changes in ice drift across leads that are a defining characteristic of winter motion in the Beaufort Sea. Comparisons between simulated and observed dynamics of the 2013 event are detailed in Supplemental Text S2 and Figures S1, S2, S3. We have collated records of events with similar synoptic forcing and ice dynamics to winter 2013 that can be used to further assess the performance of models such as neXtSIM.

For a model to accurately simulate a Beaufort breakout event the atmospheric forcing must capture the location, track and extent of anticyclones well. Small offsets in the center of the high, differences in timing or persistence of the high, and errors in ridge orientations can result in large errors in the location of lead formation and hence ice drift. While this is challenging for models, the neXtSIM team have demonstrated it is possible.

6 Open Research

The neXtSIM model output (Rheinlænder, 2022) is available at `https://doi.org/10.5281/zenodo.5639492`. NSIDC Polar Pathfinder sea ice drift (Tschudi et al., 2019) is available at `https://doi.org/10.5067/INAWUWO7QH7B`. Leads identified by Lewis and Hutchings (2019) are provided at `https://doi.org/10.1029/2018JC014898`. Leads derived from MODIS imagery (Willmes & Heinemann, 2015a, 2015b) are available at `https://doi.org/10.1594/PANGAEA.854411`. MODIS imagery (MODIS Characterization Support Team (MCST), 2017) available at `http://dx.doi.org/10.5067/MODIS/MOD021KM.061`. ERA5 atmospheric reanalysis (Hersbach et al., 2018) available at `https://doi.org/10.24381/cds.adbb2d47`.

Acknowledgments

The authors have been supported by NASA grants 80NSSC18K1026 and 80NSSC21K1601. We thank Ben Lewis and Lew Shapiro for their conversations with us identifying correspondence between Beaufort lead patterns and the progression of anticyclones. We thank Jonathan Rheinlænder and Einar Ólason for sharing model output and information that has furthered the discussion started in Rheinlænder et al. (2022).

References

Babb, D. G., Landy, J. C., Barber, D. G., & Galley, R. J. (2019). Winter sea ice export from the Beaufort Sea as a preconditioning mechanism for enhanced summer melt: A case study of 2016. *Journal of Geophysical Research: Oceans*, *124*, 6575–6600. doi: 10.1029/2019JC015053

The cracks of dawn. (2013). `https://neven1.typepad.com/blog/2013/03/the-cracks-of-dawn.html#more`. (Accessed: 2022-06-22)

Hersbach, H., Bell, B., Berrisford, P., Biavati, G., Horányi, A., Muñoz Sabater, J., ... Thépaut, J.-N. (2018). *Era5 hourly data on single levels from 1959 to present* [dataset]. Copernicus Climate Change Service (C3S) Climate Data Store (CDS). Retrieved from `https://doi.org/10.24381/cds.adbb2d47` (Accessed: 2022-06-22) doi: 10.24381/cds.adbb2d47

Lewis, B. J., & Hutchings, J. K. (2019). Leads and associated sea ice drift in the Beaufort Sea in winter. *Journal of Geophysical Research: Oceans*, *124*, 3411–3427. doi: 10.1029/2018JC014898

MODIS Characterization Support Team (MCST). (2017). *Modis 1km calibrated radiances product* [dataset]. NASA MODIS Adaptive Processing System, Goddard Space Flight Center, USA. Retrieved from `http://dx.doi.org/10.5067/MODIS/MOD021KM.061` (Accessed: 2022-06-22) doi: 10.5067/MODIS/MOD021KM.061

Rheinlænder, J. W. (2022). *nextsim-data-breakup2013-beaufortsea* [dataset]. Zenodo. Retrieved from `https://doi.org/10.5281/zenodo.5639492` (Accessed: 2022-06-22) doi: 10.5281/zenodo.5639492

Rheinlænder, J. W., Davy, R., Ólason, E., Rampal, P., Spensberger, C., Williams, T. D., ... Spengler, T. (2022). Driving mechanisms of an extreme winter sea ice breakup event in the Beaufort Sea. *Geophysical Research Letters*, *49*(e2022GL099024). doi: 10.1029/2022GL099024

Tschudi, M., Meier, W. N., Stewart, J. S., Fowler, C., & Maslanik, J. (2019). *Polar pathfinder daily 25 km ease-grid sea ice motion vectors, version 4* [dataset]. Boulder, Colorado USA. NASA National Snow and Ice Data Center Distributed Active Archive Center. Retrieved from `https://doi.org/10.5067/INAWUWO7QH7B` (Accessed: 2022-06-22) doi: 10.5067/INAWUWO7QH7B

Willmes, S., & Heinemann, G. (2015a). Pan-arctic lead detection from MODIS thermal infrared imagery. *Annals of Glaciology*, *56*(69), 29–37. doi: 10.3189/

2015AoG69A615
Willmes, S., & Heinemann, G. (2015b). Sea-Ice Wintertime Lead Frequencies and Regional Characteristics in the Arctic, 2003–2015. *Remote Sensing*, *8*(1), 4. doi: 10.3390/rs8010004